Structural Study of the Relationship between the Rate of Membrane Fusion and the Ability of the Fusion Peptide of Influenza Virus To Perturb Bilayers†

A. Colotto and R. M. Epand*

Department of Biochemistry, McMaster University, Health Sciences Centre, 1200 Main Street West, Hamilton, Ontario, Canada L8N 3Z5

Received February 19, 1997; Revised Manuscript Received April 11, 1997⊗

ABSTRACT: The amino-terminal segment of the HA_2 protein of influenza virus (fusion peptide) has been identified as an important region for membrane fusion. The wild type virus can fuse to membranes more rapidly at pH 5 than at pH 7.4. It has been demonstrated that there is a relationship between the ability of the peptide to promote the formation of inverted phases and the fusogenicity of the intact virus. In this work, we use small-angle X-ray diffraction to study the mechanism of the structural effect of the peptide, at different pHs, on lipid systems characterized by each having a different spontaneous radius of curvature. The overall results show that the action of the peptide on the polymorphism of the lipid systems investigated is strongly pH-dependent. In particular, a rapid formation of cubic phases at pH 5.0 is observed in the presence of this fusion peptide. The ability of the fusion peptide to promote cubic phases exhibits the same dependence on the pH as does the fusogenicity of the intact virus. It is proposed that the peptide promotes cubic phases at pH 5.0 by changing the kinetics of the lamellar to inverted phase transitions.

The fusion of influenza virus to cells and liposomes has been extensively studied. The hemagglutinin (HA) protein of the envelope of this virus is the best-characterized viral fusion protein. This protein is activated to become fusogenic by proteolytic cleavage into two disulfide-linked glycopolypeptides, HA_1 and HA_2. These fragments self-associate to form a 220 kDa trimer of identical subunits. The structural features of this trimer are known from the X-ray crystallographic studies of Wiley and co-workers. This group has determined the structure of the ectodomain of the HA protein at neutral pH to 2.2 Å resolution (Wilson et al., 1981; Watowich et al., 1994). Although there is evidence that influenza fusion occurs at neutral pH (Haywood & Boyer, 1985), at an endosomal pH of 5−6, the fusion rate of the wild type influenza virus is greatly enhanced (Gething et al., 1986). At acidic pH, this bromelain-cleaved ectodomain of the HA protein aggregates and cannot be crystallized. However, through truncation of this fragment, through removal of 37 amino acid residues from the amino terminus of the HA_2 fragment, the crystal structure could be solved (Bullough et al., 1994). The 37-amino acid fragment that is removed contains the so-called fusion peptide that has been identified as an important region for membrane fusion (Gething et al., 1986). Photolabeling studies indicate that this fusion peptide inserts into the target membrane (Durrer et al., 1996). It has recently been suggested that the fusion peptide facilitates the expansion of the fusion pore (Schoch & Blumenthal, 1993).

There are at least two pH-dependent phenomena that can contribute to the enhanced rate of fusion at acidic pH. One is a pH-dependent conformational change in the HA protein involving either the formation of a coiled coil at low pH (Carr & Kim, 1993) or a change in the angle at which the HA protein protrudes from the membrane to allow for closer juxtaposition of the two apposing membranes (Tatulian et al., 1995). There is recent evidence to suggest that there is considerable conformational flexibility in both the neutral and acidic forms of the HA protein, suggesting that the coiled coil model may be an oversimplification (Kim et al., 1996). The other pH-dependent process is the protonation of the acidic amino acid side chains in the fusion peptide. There have been a number of studies demonstrating that the influenza fusion peptide is more disruptive to membrane bilayers at acidic pH than at neutral pH (Wharton et al., 1988; Burger et al., 1991; Murata et al., 1991; Rafalski et al., 1991; Epand et al., 1992; Düzgünes & Shavnin, 1992). Thus, both the protonation of the fusion peptide and conformational changes in the intact HA protein trimer may contribute to the pH dependence of influenza fusion.

In this work, we further explore the effect of the influenza fusion peptide on membrane properties at different pH values. It has been demonstrated that there is a relationship between the ability of this peptide to promote the formation of inverted phases and the fusogenicity of the intact virus (Epand & Epand, 1994). Of course, the peptide is a very simplified model of the intact fusion protein and certainly of the intact virus. The fusion peptide is not likely to bridge two membranes, and it has no receptor binding function. Furthermore, the isolated peptide may differ from this segment in the intact protein in its conformation, depth of insertion into the lipid membrane, and subunit association. Nevertheless, viral fusion peptides have membrane-perturbing properties which suggest that they mimic, at least certain aspects of, the fusion of intact viruses.

Although proteins may be the main regulators of biomembrane fusion events, determining when and where membrane fusion occurs (Burger & Verkleij, 1990; Stegmann et al., 1989), the central event during membrane fusion is the merger of two membranes, which requires a transient

† This work was supported by Grant MT 7654 from the Medical Research Council of Canada.

* To whom requests for reprints should be addressed. E-mail: Epand@fhs.csu.McMaster.CA.

⊗ Abstract published in *Advance ACS Abstracts,* June, 1, 1997.

S0006-2960(97)00382-6 CCC: $14.00

reorganization of membrane lipids (Burger, 1997). Therefore, lipids are likely to play a key role in the induction of biomembrane fusion. Membrane lipids play a role in both the binding of viruses and subsequent viral fusion (Epand et al., 1995). It is thus difficult to assess the role of lipid in the membrane fusion step by monitoring the overall rate of fusion. Nevertheless, it is clear that viruses can fuse to many different bilayer membranes with different chemical structures and physical properties (Stegmann, 1993). Hence, it may be the local arrangement of lipid around the fusion peptide that determines the rate of fusion.

It has been suggested that a prerequisite of the fusogenicity of fusion sequences is their oblique insertion into the membrane, increasing the intrinsic negative curvature of the bilayer (Martin et al., 1994; Epand & Epand, 1994; Colotto et al., 1996). There is disagreement about the nature of the insertion of the influenza fusion peptide into membranes. In one study, it has been shown that the HA_2 fusion sequence penetrates into a hydrophobic environment at an oblique angle independent of pH (Lüneberg et al., 1995), while another study indicates that at acidic pH a related peptide lies with its helical axis parallel to the membrane surface (Ishiguro et al., 1996). Therefore, it remains unclear what characteristics of this lipid−peptide interaction determine the membrane-disrupting action of the fusion peptide.

MATERIALS AND METHODS

Sample Preparation. The lipids monomethyldioleoylphosphatidylethanolamine (MeDOPE),[1] (lot 181mpe-53) and dipalmitoleoylphosphatidylethanolamine (DPoPE) (lot 161pe-16) were purchased from Avanti Polar Lipids (Alabaster, AL). Lipids were used without further purification.

The fusion peptide of the X31 strain of influenza virus, with the sequence GLFGAIAGFIENGWEGMIDG-amide, was synthesized by the Macromolecular Structure Analysis Facility of the University of Kentucky, using standard solid phase synthetic methods. The final purification of the peptide was on a Whatman, Magnum 9, Partisil 10 ODS-3, C_{18} reverse phase column. The identity of the peptide was verified by fast bombardment mass spectrometry and by amino acid analysis.

Lipid films were prepared from $CHCl_3$/MeOH (2:1) solution by solvent evaporation under nitrogen. For samples containing peptide, the peptide was dispersed in the lipid solution of organic solvent and the mixture was vigorously vortexed until a homogeneous solution could be achieved. The solvent was then evaporated as for the pure lipid. In order to remove residual traces of the solvent, samples were placed under vacuum for 2 h and then lyophilized overnight. The films were subsequently hydrated by adding a 4-fold weight excess of the desired buffer: 10 mM citrate and 0.15 M NaCl at pH 5.0 or 20 mM PIPES, 1 mM EDTA, and 150 mM NaCl with 0.002% NaN_3 at pH 7.4. The lipid was suspended by vortexing repeatedly at room temperature over a period of 1 h.

[1] Abbreviations: *R*, peptide to lipid molar ratio; R_0, spontaneous radius of curvature; MLV, multilamellar vesicles; MeDOPE, monomethyldioleoylphosphatidylethanolamine; DPoPE, dipalmitoleoylphosphatidylethanolamine; T_H, bilayer to hexagonal phase transition temperature; Q, cubic phase; H_{II}, hexagonal phase; L_α, liquid crystalline lamellar phase.

X-ray Diffraction Experiments. Nickel-filtered CuKα (λ = 1.54 Å) X-rays were obtained from a Rigaku-Denki rotating anode. X-rays were focused using a Frank's type camera and recorded using a position-sensitive proportional counter (TEC model 205) (Sen et al., 1990). Unoriented lipid dispersions, prepared as described above, were measured in 1.5 mm ∅ glass capillaries for all diffraction experiments. The samples were centrifuged in the capillaries. The same heating protocol was used for samples with and without peptide. The specimen temperature (± 0.5 °C) during X-ray diffraction measurements was controlled by a thermoelectric device. For the measurement of lattice spacing vs temperature, the typical protocol involved stepwise heating of the specimen in intervals of 10 °C in the temperature range of the L_α phase, in intervals of 1−2 °C in the proximity of the bilayer to hexagonal phase transition temperature T_H, and then again in intervals of 10 °C above T_H. The systems were allowed to equilibrate for about 5 min at the desired temperature before measurement. The X-ray exposure times were typically 10−15 min. It should be noted that these diffractograms must be symmetrical for the nonoriented samples we are using. Deviations from a symmetrical pattern are largely due to position-dependent variations in detector efficiency but in special cases could also occur if large cubic phase crystallites were oriented by the capillary itself. The center of all of the diffractograms have two large positive peaks on either side of a deep trough. This pattern is a normal consequence of the presence of the beam stop and is not a result of diffraction by the sample. Because of the small size of the figures, some of the higher, weaker orders cannot easily be seen in the figure but are readily observed in the original data and are referred to in the text.

The spacing of the peaks in the diffractograms allows us to specify the nature of the packing symmetry of the phase, *i.e.*, L, Q, or H (lamellar, cubic, or hexagonal), while the distance of peaks from the center of the symmetrical powder pattern allows us to calculate the repeat or *d* spacing of that phase. This is done, after baseline subtraction for all of the easily resolvable orders, and the calculated *d* spacing is given as an average of these values. Typical absolute lattice spacings, calibrated against freshly crystallized nonadecane (d = 26.2 Å), are accurate to ±0.5 Å for lattices up to ∼80 Å and to ±1−2 Å for larger lattices.

RESULTS

MeDOPE. Fully hydrated dispersions of MeDOPE are found to form different ordered structures, *i.e.*, lamellar, cubic (*Pn*3 or *Pn*3*m*), or hexagonal, depending on both the temperature and thermal history of the sample (Gruner et al., 1988; Siegel & Banschbach, 1990; Gagne et al., 1985; Silvius & Brown, 1986; van Gorkom et al., 1992). The cubic structures are observed, or not, as stable or metastable phases between the lamellar and hexagonal phases. This depends on the time scale of the temperature scan across the lamellar to hexagonal phase transition (van Gorkom et al., 1992). If the sample is heated relatively fast (40 °C/h), the system will undergo a phase transition from the liquid crystalline lamellar phase (L_α) to a type II hexagonal phase (H_{II}) at T_H (T_H is found to vary between 60 and 66 °C, depending on the sample purity and concentration). If the system is heated relatively slowly (<13 °C/h), it will undergo a phase

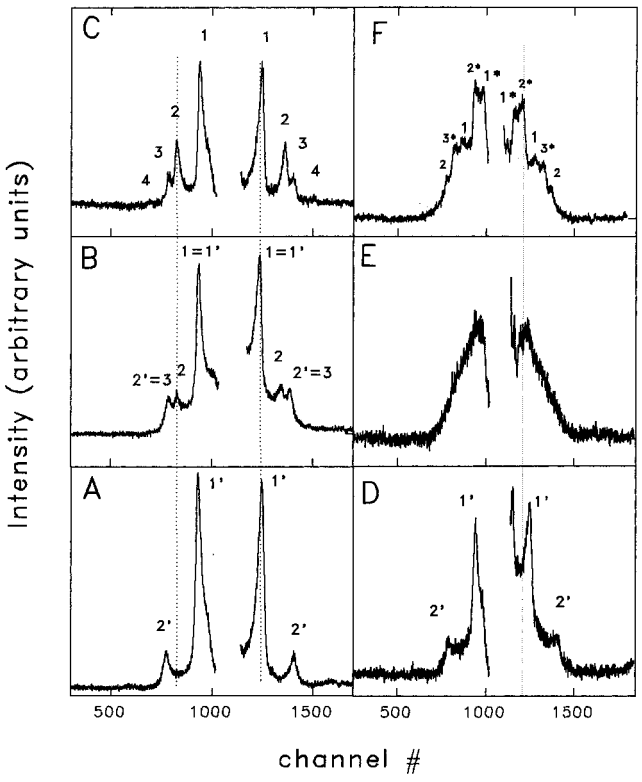

FIGURE 1: Typical small-angle X-ray diffraction profiles obtained for MeDOPE systems at pH 5.0, with and without peptide, and at different temperatures: (A) lipid without peptide below $T_H = 60$ °C; (B) lipid without peptide at T_H; (C) lipid without peptide above T_H; (D) MeDOPE/flu peptide, $R = 10^{-2}$, at $T < 50$ °C; (E) MeDOPE/flu peptide, $R = 10^{-2}$, at 55 °C $\leq T \leq$ 69 °C; and (F) MeDOPE/flu peptide, $R = 10^{-2}$, at $T = 80$ °C.

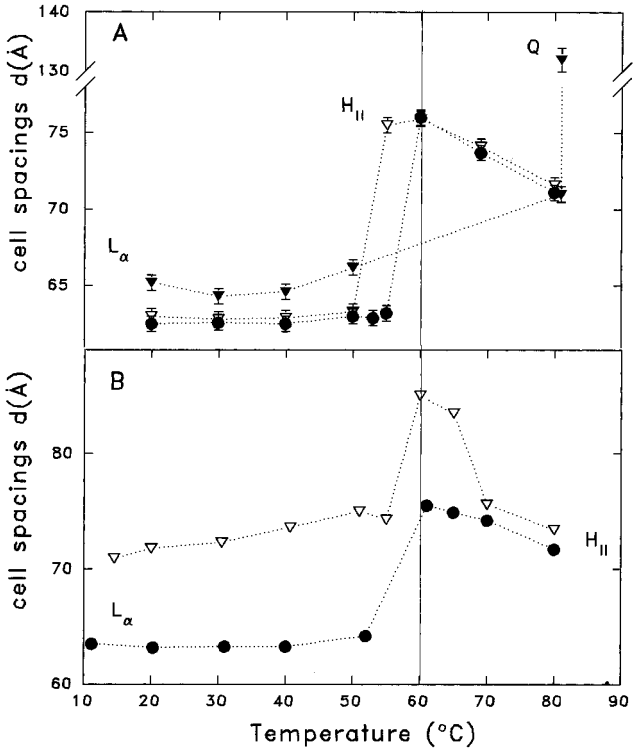

FIGURE 2: Crystallographic data calculated from X-ray diffractograms of MeDOPE at pH 5.0, obtained upon gradual heating of the sample. The *d* spacings are plotted vs temperature: (A) pH 5.0, (●) $R = 0$, (▽) $R = 10^{-3}$, and (▼) $R = 10^{-2}$; and (B) pH 7.4, (●) $R = 0$ and (▽) $R = 10^{-2}$.

transition from the lamellar to a cubic phase at a temperature lower than T_H. The L_α to cubic phase transition was verified for this system by slow-scan differential scanning calorimetry and static-temperature X-ray diffraction at closely spaced temperature intervals (Siegel & Banschbach, 1990). It has also been reported that the thermotropic phase behavior of this system, as well as its structural dimensions, is highly concentration-dependent (Gruner et al., 1988). In the experiments reported below, the samples have been handled so as to have the pure MeDOPE transiting directly from the lamellar to the hexagonal phase. For our samples, this occurred at $T_H \sim 60$ °C, in agreement with other values in the literature. Cooling scans show H_{II} phase down to about 55 °C. It is generally found that the hexagonal to lamellar phase transition exhibits some hysteresis on cooling (Epand & Epand, 1988). Also, samples containing the influenza peptide show a lower T_H in heating scans. The samples were treated in a systematic manner in order to assure reproducibility and for the sake of comparison.

X-ray diffractograms obtained for MeDOPE at pH 5.0 are shown in Figure 1A−C. Under the experimental conditions used, only the first four order reflections of the lamellar phase (*d* spacing ratio of 1:2:3:4:...) were observed (Figure 1A, the third and fourth orders are clearly seen in the original data). The system transits to the hexagonal phase in what we refer to as an "ordered way". By this, we mean that, in the temperature range where the phase transition takes place, lamellar phase domains coexist with hexagonal phase domains. Due to phase coexistence, diffraction peaks from both phases are observed around the phase transition temperature (Figure 1B). Using our heating protocol (see Materials and Methods), we did not observe the formation of the cubic phase with the pure lipid. It should be noted, however, that this phase has been observed by other authors using a different heating regime with closely spaced temperature intervals (Siegel & Banschbach, 1990). Figure 1C shows a typical diffractogram obtained for the H_{II} phase. Five diffraction peaks are observed (*d* spacing ratio of $1{:}\sqrt{3}{:}\sqrt{4}{:}\sqrt{7}{:}\sqrt{9}{:}...$). As the temperature is increased, the reflections shift to higher angles, indicating that the hexagonal phase cell parameter decreases (Figure 2A, filled circles). This is a typical result for H_{II} phases and is due to the volume of the hydrophobic moieties of the lipids increasing with increased temperature, producing changes in spontaneous curvature at the interface. Our X-ray diffraction results for the pure lipid system in the lamellar and hexagonal phases are in agreement with previously published data (Gruner et al., 1988). The detection of the coexistence of lamellar and hexagonal domains may be facilitated by the slow rate of water penetration into the forming H_{II} phase. The transition occurs much more rapidly when starting with LUV instead of MLV (Siegel & Epand, 1997).

At pH 7.4, the pure lipid system behaves in the same way as it does at pH 5.0. The diffractograms obtained (data not shown) are equal to those obtained at lower pH, and the structural parameters are the same (Figure 2B, filled circles).

MeDOPE and Fusion Peptide. The effects of adding the HA fusion peptide to MeDOPE multilamellar systems are strongly dependent on the pH. At pH 5.0 and a low peptide to lipid molar ratio, $R = 10^{-3}$, the diffraction patterns obtained are similar to those for the lipid alone (data not shown). However, the transition from lamellar to hexagonal

Table 1: Crystallographic Data Calculated from Diffractograms Obtained from the MeDOPE/flu Fusion Peptide ($R = 10^{-2}$) System at pH 5.0 at 80 and 70 °C while Heating and Cooling the Samples, Respectively[a]

heated up sample					cooled down sample					literature	
	cubic		hexagonal			cubic		hexagonal		cubic	
d_{meas} (Å)	$h^2+k^2+l^2$	d_{calc} (Å)	h^2+k^2+hk	d_{calc} (Å)	d_{meas} (Å)	$h^2+k^2+l^2$	d_{calc} (Å)	h^2+k^2+hk	d_{calc} (Å)	$h^2+k^2+l^2$	d (Å)
95.6	2	93.3	–	–	96.5	2	96.9	–	–	2	96.2
73.3	3	76.2	–	–	78.8	3	79.1	–	–	3	78.5
61.4	4	66.0	1	61.5	63.2	4	68.5	1	63.2	4	68.0
	6	53.9			6	55.9					
43.4	9	44.0	–	–	46.5	9	45.7	–	–	6	55.5
35.6	14	35.3	3	35.5	36.9	14	36.6	3	36.5	8	48.1
30.7	19	30.3	4	30.8	31.4	19	31.4	4	31.6	9	45.3
	$a_{calc} = 132$ Å		$d_H = 71$ Å			$a_{calc} = 137$ Å		$d_H = 73$ Å		$a = 136$ Å	

[a] In both cases, the cubic phase coexists with the hexagonal phase. Data obtained for the pure lipid system, when the sample was submitted to a special thermal treatment, are also listed for comparison (Gruner et al., 1988).

phase occurs at a lower temperature in the presence of 0.1% peptide ($T_H = 55$ °C) (Figure 2A, open triangles). It is interesting to note that, although the transition temperature is lowered, the *d* spacings are not changed. At $R = 10^{-2}$, the peptide decreases the stacking order of the liquid crystalline lamellar phase, L_α, as can be seen from the broadening of the diffraction peaks (Figure 1D). In addition, at $T = 55$ °C, the reflections corresponding to the lamellar phase evolve into a continuous scattering curve characteristic of a highly disordered structure. This continuous scattering curve persists up to about 80 °C, when diffraction peaks can be distinguished as corresponding to a cubic phase coexisting with a hexagonal phase (Figure 1F). The crystallographic data calculated from this diffractogram are listed in Table 1. The calculated cell parameter of the hexagonal phase, $d_H = 71$ Å, is the same as the one obtained for the pure lipid system at this same temperature (Gruner et al., 1988). The calculated cell parameter of the cubic phase (symmetry group *Pn*3*m*), $a = 132$ Å, is very close to the one reported in the literature for the pure lipid, a = 136 Å (Gruner et al., 1988). These results are in agreement with the ^{31}P NMR data reported in a previous work on the dependence of pH on the effects of the influenza virus fusion peptide on MeDOPE (Epand & Epand, 1994). In particular, it was found that for pH 5.0 the peptide converted the ^{31}P NMR powder pattern completely into an isotropic signal at all temperatures between 45 and 60 °C.

Since it is known that the hysteresis in the polymorphic phase behavior of MeDOPE is strongly dependent on the temperature scan rate, we investigated the effects of the peptide when the system is taken from room temperature directly to 80 °C and then cooled (Figure 3). The pure lipid and the peptide-containing system both convert from the L_α phase to the H_{II} phase when the temperature is raised from 20 to 80 °C in a single step. However, while the pure lipid system preserves the hexagonal symmetry when the temperature is lowered, the peptide-containing sample undergoes a phase transition to a cubic phase. The cubic phase persists down to 45 °C, although it is very disordered. Below 40 °C, the reflections characteristic of the L_α phase become visible for the peptide-containing specimen. When no peptide is present, the system takes a very long time to reorder in the lamellar phase. The pure MeDOPE becomes very disordered at T_H, and the lamellar phase does not reform on cooling to temperatures as low as 35 °C [in agreement with previous observations reported by Gruner et al. (1988)]. The crystallographic data of the cubic phase observed for the peptide-containing system at 70 °C, as the sample was cooled, are listed in Table 1. The cell parameter and symmetry group of this cubic phase are the same as those observed for the peptide-containing specimen upon heating and for the pure lipid system when submitted to a special thermal treatment (Gruner et al., 1988), respectively.

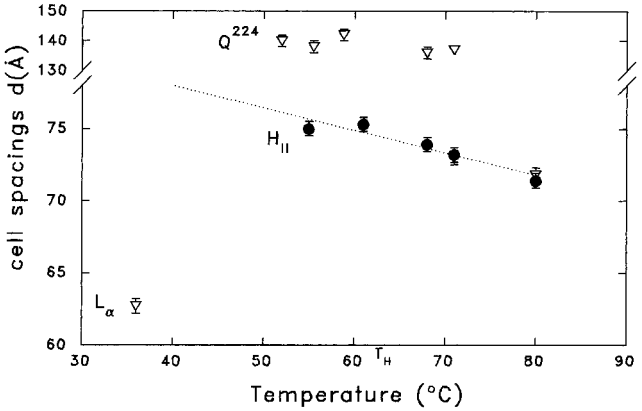

FIGURE 3: Crystallographic data calculated from X-ray diffractograms obtained upon cooling of the sample at pH 5.0 after rapid heating to 80 °C. The *d* spacings are plotted vs temperature: (●) $R = 0$ and (▽) $R = 10^{-2}$.

At pH 7.4, the $L_\alpha - H_{II}$ phase transition temperature of MeDOPE is not changed by the peptide (Figure 2B). However, the lamellar repeat distance increases by about 8 Å at $R = 10^{-2}$. The cell spacing of the hexagonal phase, d_H, increases by about 10 Å when *T* is between 50 and 65 °C, but at higher temperatures, it is only slightly larger than that observed for the pure lipid system. It is noteworthy that, in the temperature range at which d_H is much larger, the system is very disordered.

DPoPE. In the temperature range investigated in this work (15−80 °C), pure DPoPE presents one phase transition, from the L_α to a type II hexagonal phase at $T_H = 43.2$ °C (Epand, 1990). We have recently published diffraction data from this lipid (Colotto et al., 1996). The diffraction curves show the characteristic profiles for the L_α (Figure 4A), the hexagonal phase (Figure 4C), and phase coexistence at about T_H (Figure 4B). These data at pH 5.0 are in good agreement with our previous results (Colotto et al., 1996) measured at pH 7.4. The low T_H, and the relatively small hexagonal phase *d* spacing, d_H (Figure 6) of the DPoPE system, compared to those of the MeDOPE system, indicate that the former has a smaller intrinsic radius of curvature, R_0. Another remarkable difference between DPoPE and Me-

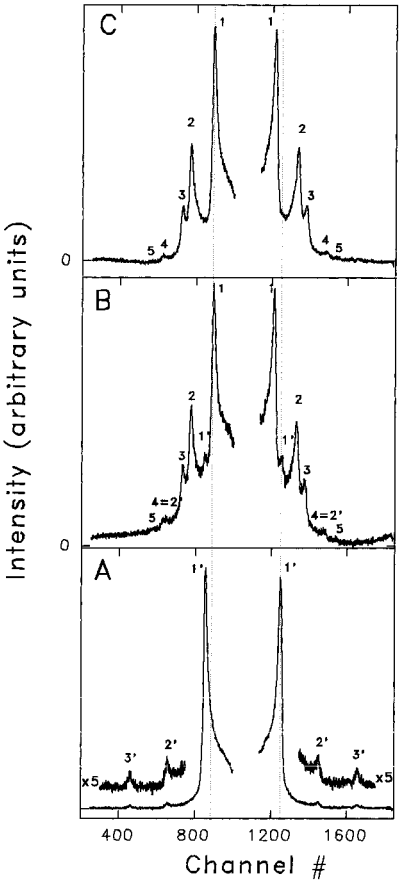

FIGURE 4: Typical small-angle X-ray diffraction profiles obtained for the DPoPE system without peptide at pH 5.0: (A) system below $T_H = 40$ °C, (B) system at T_H, and (C) system above T_H. The labels 1−3 indicate the reflections due to the lamellar liquid crystalline phase, and the labels 1′−3′ indicate the reflections due to the H_{II} phase. Part curve A has been amplified by a factor of 5 for the sake of clarity.

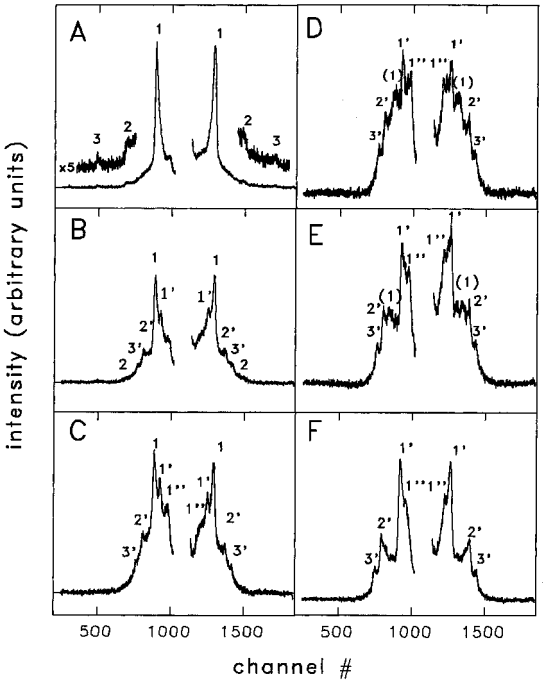

FIGURE 5: Typical X-ray diffractograms obtained for the system DPoPE/flu peptide at pH 5.0, and with $R = 10^{-2}$: (A) $T = 30$ °C, (B) $T = 40$ °C, (C) $T = 42$ °C, (D) $T = 50$ °C, (E) $T = 60$ °C, and (F) $T = 70$ °C. The labels 1−3 indicate the reflections due to the lamellar liquid crystalline phase; the labels 1′−3′ indicate the reflections due to the H_{II} phase, and the label 1″ indicates the reflection due to the cubic phase. Part of curve A has been amplified by a factor of 5 for the sake of clarity.

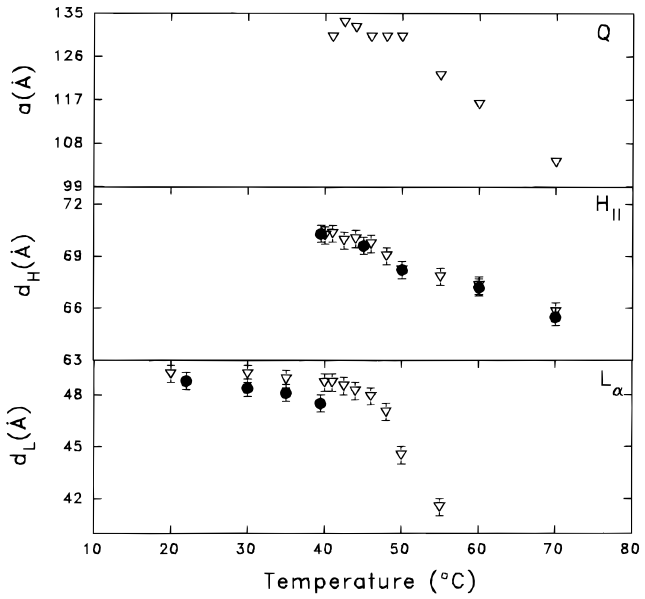

FIGURE 6: Crystallographic data calculated from the diffractograms obtained for the DPoPE system at pH 5.0. The lattice parameters are grouped according to the corresponding phase. In certain conditions, phase coexistence was observed: (●) $R = 0$ and (▽) $R = 10^{-2}$.

DOPE lies in the fact that DPoPE has stronger hydrogen bonding among the lipid polar head groups, and is therefore less hydrated (Rand et al., 1988). This explains the smaller lamellar repeat distance in DPoPE as compared to that in MeDOPE (Figure 6).

DPoPE and Fusion Peptide. The peptide effects on the DPoPE polymorphic behavior are strongly dependent on the pH, just as for MeDOPE. At pH 5.0, below T_H, the peptide-containing system is found in a lamellar phase with a *d* spacing similar to that of the pure lipid system (Figure 6). However, the stacking disorder is higher when the peptide is present (this is seen from the broadening of the diffraction peaks, most evident for the second and third order reflections, *viz.*, Figure 5A vs Figure 4A). In addition, the temperature dependence of the lamellar *d* spacing in the presence of the peptide is slightly different from the pure lipid one (see Figure 6). At 40 °C (Figure 5B), reflections characteristic of the hexagonal phase appear together with the lamellar phase ones. At 42 °C (Figure 5C), the first order reflection of a third phase is observed. This reflection seems to already be present at 30 °C, but it becomes really well resolved above 42 °C. It is not possible to determine the exact nature of the structure giving rise to this peak; however, its presence is reproducible in different, independently prepared samples. On the basis of the large *d* spacing, we speculate that it is due to a cubic phase. The DPoPE system has not been as thoroughly studied as the MeDOPE, and to our knowledge, the observation of a cubic phase for this lipid has not been previously reported. Nevertheless, it has been suggested that cubic phases can be induced in any lipid system presenting an $L_\alpha - H_{II}$ phase transition (Shyamsunder et al., 1988). The three phases persist up to 55 °C. At this temperature, the L_α phase vanishes. The *d* spacing of the lamellar phase decreases with increasing temperature throughout its existence range. In particular, above T_H, this dependence

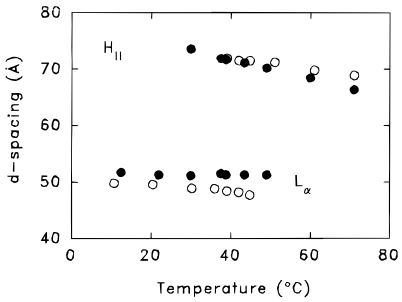

FIGURE 7: Crystallographic data calculated from the diffractograms obtained for the DPoPE system at pH 7.4: (○) $R = 0$ and (●) $R = 10^{-2}$.

becomes very strong (Figure 6). The H_{II} phase and the third phase, assumed to be a cubic phase, persist up to the higher temperature studied (Figures 5D−F and 6). The peptide does not affect the lattice cell parameter, d_H, of the hexagonal phase. Neither is the temperature dependence of d_H changed. The cell parameter, *a*, of the cubic phase varies with the temperature in a manner analogous to that of the hexagonal phase; *i.e.*, the cell parameter decreases with increasing temperature (Figure 6).

For the sake of comparison, we studied the peptide effect on the DPoPE system at pH 5.0 upon cooling the system, after sudden heat. Absolutely no differences were observed between the polymorphic behavior of the pure lipid and the peptide-containing one upon cooling (data not shown).

At pH 7.4, a most striking effect of the peptide on the lipid phase behavior is the broadening of the range of temperatures over which phase coexistence is observed (Figure 7). Moreover, the *d* spacing of the lamellar phase does not decrease with temperature (contrary to the pure lipid system), and the dependence of the *d* spacing of the hexagonal phase on the temperature is slightly affected.

DISCUSSION

The influenza fusion peptide is found to increase the lamellar *d* spacing, d_L, of both MeDOPE and DPoPE and at both pHs (Figures 2, 6, and 7). The increase is significantly greater at pH 7.4 than at pH 5.0. This is in agreement with the peptide more strongly pushing apart the bilayers at higher pH because of the higher negative charge on the peptide. The increase in d_L is more dramatic for MeDOPE than for DPoPE, perhaps because the peptide is more effective in increasing the hydration of MeDOPE than it is with DPoPE.

Similarly, d_H of MeDOPE at pH 7.4 is also increased by the presence of the peptide. The observed hexagonal phase is disordered. A likely cause for this disordering is the concomitant formation of interlamellar attachment sites and cubic phase domains which break up the H_{II} phase domains into smaller aggregates, resulting in broader X-ray reflections. There is direct evidence for the coexistence of the H_{II} phase and such defects (Siegel et al., 1994). The stabilization of the H_{II} phase at higher temperatures, which is accompanied by a dramatic decrease in d_H (Figure 2B), must result from a reordering of the peptide along the cylinders with consequent lowering of the electrostatic repulsion. At pH 5.0, where there is less charge on the peptide, there is also less effect on d_H (Figure 2A). Again, as with d_L, the d_H of DPoPE is less affected than MeDOPE by the peptide at pH 7.4 (Figure 7), and d_H of DPoPE is not affected at all at pH 5.0 (Figure 6).

Negative curvature strain in membranes has been associated with increased rates of membrane fusion. In the case of viral fusion, there is evidence that amphiphiles which raise the bilayer to hexagonal phase transition temperature of model lipids inhibit the rate of viral fusion (Epand, 1992; Cheetham et al., 1994; Chernomordik, 1996). In addition, viral fusion peptides lower the T_H of DPoPE (Epand & Epand, 1994; Epand et al., 1994). In the case of the influenza fusion peptide studied here, T_H is lowered only under fusogenic conditions at acidic pH (Epand & Epand, 1994) but d_H is not altered (Figures 2 and 6). In comparison, the SIV fusion peptide reduces the d_H of MeDOPE, indicating that it increases negative monolayer curvature; *i.e.*, it reduces R_0 (Colotto et al., 1996). Perhaps a change in d_H is not observed in the present case with the influenza fusion peptide because it contains several acidic amino acid residues which would retain a partial charge even at the acidic pH of 5.0. The resulting charge repulsion may prevent the small decrease in d_H observed with the uncharged and very hydrophobic SIV peptide. Nevertheless, the lack of correlation between the bilayer-destabilizing action of the influenza fusion peptide and the promotion of negative curvature suggests that other factors may be involved.

An additional consideration is the membrane sidedness dependence of curvature effects on fusion rates (Chernomordik, 1996). According to the stalk−pore hypothesis, negative curvature in the contacting monolayers will increase fusion rates, while in the distal monolayers, it will decrease the rate of fusion. In the case of the fusion peptide segment of an intact virus, there is little evidence to indicate how deeply it inserts into a target membrane. For the peptide/lipid mixtures studied in the present work, the fusion peptide has equal access to both monolayers of the bilayer.

A most striking effect of the fusion peptide is the formation of a cubic phase, which occurs only at pH 5.0 in the presence of peptide for both lipid systems (see Results). This observation demonstrates that the curvature modulation effect of this fusion peptide is strongly pH-dependent and increases at acidic pH as do the effects of the peptide and the intact virus on membranes. At pH 5.0, for MeDOPE, the L_α phase is already destabilized at $T > 55$ °C for $R = 10^{-3}$. At high peptide contents, the formation of the hexagonal phase is shifted to higher temperatures. The system remains very disordered up to 80 °C, and at this temperature, a cubic phase coexists with the hexagonal one. For DPoPE, at T_H, in the presence of the peptide, not only is the H_{II} phase observed, but also traces of the lamellar phase and of a cubic phase. The three phases (L, Q, and H) coexist over a broad temperature range; the lamellar phase vanishes, and finally, at 80 °C, only traces of the Q phase remain.

The induction of a cubic phase in the DPoPE system is particularly interesting since a cubic phase has never been previously observed for this lipid. Moreover, as judged from the dimension of the hexagonal phase *d* spacing, the spontaneous radius of curvature, R_0, of this lipid is relatively small. It is also true that the acyl chain length of this lipid is slightly shorter than that for MeDOPE; however, this factor is not expected to have a marked effect either on the position of the pivotal plane or on R_0. Dioleoylphosphatidylethanolamine, which has acyl chains that are two carbons longer than DPoPE, also has a lower hexagonal phase *d* spacing than MeDOPE (Epand et al., 1996). In addition, DPoPE has a much lower T_H, indicating that it has a low R_0. Cubic

phase transitions have been more frequently observed in systems which are characterized by an intermediate spontaneous curvature (Anderson et al., 1988). However, it has been suggested that cubic phases can be induced in any lipid system presenting an $L_\alpha-H_{II}$ phase transition. In fact, it has been shown that a cubic phase can be also induced in dioleoylphosphatidylethanolamine by extensive thermal cycling (Shyamsunder et al., 1988).

We suggest that the formation of a cubic phase at pH 5.0 is due to an effect of the peptide on the kinetics of the transition for both lipid systems. This is in agreement with the idea that the difficulty involved in settling a system into or out of a cubic phase is due to a relatively large kinetic energy barrier separating this phase from both the lamellar and hexagonal phases (Shyamsunder et al., 1988). It is also noteworthy that, although for the DPoPE system, the cubic phase coexists with the hexagonal phase, the R_0 of the later is exactly the same as that of the system without peptide (Figure 6). Of course, phase separation with domains rich in peptide and domains poor in peptide could be suggested, but then why would the lamellar phase persist up to temperatures as high as 55 °C (almost 15 °C above T_H)? The results suggest that the influenza fusion peptide has more effect on the transition to the cubic phase by promoting the rate of this transition than it has on the hexagonal phase and that this kinetic effect occurs only at pH 5.0 where the virus is more fusogenic.

The presumed role of the fusion peptide is to facilitate the kinetics of membrane fusion and therefore lower the activation energy for steps in the fusion process, rather than having a thermodynamic effect in stabilizing a particular structure. The pathway for membrane fusion is not likely to involve the formation of any novel phases but rather to proceed via specific fusion intermediates. A specific scheme for membrane fusion has been suggested (Siegel, 1993). One of the intermediates in this scheme is the interlamellar attachment (ILA) or fusion pore (Markin et al., 1984; Siegel, 1993; Chernomordik et al., 1987). There is a relationship between ILAs and the cubic phase in that ILAs have been shown by cryotransmission electron microscopy to assemble into cubic phases (Siegel et al., 1989). It has been suggested that the fusion of bilayers and the conversion of bilayers to an inverted cubic phase both proceed through the same intermediates (Siegel, 1986). This intermediate is the trans monolayer contact (TMC) (Siegel, 1993). As suggested by Siegel (personal communication), for systems with low bilayer rupture tension, the TMCs collapse into ILAs (fusion pores). These ILAs can then associate to form inverted cubic phases. In systems with higher values of the bilayer rupture tension, the TMCs do not rupture as rapidly to form ILAs, and as a result of their higher concentration, they can aggregate and elongate directly into H_{II} phase domains. It is possible that the role of the influenza fusion peptide is to decrease the rupture tension of the bilayer, thus favoring the fusion/cubic phase route, rather than the formation of the H_{II} phase. There is a precedent showing that hydrophobic peptides comprised of 16 or 24 Leu residues bound at the N and C termini by Lys can reduce vesicle rupture tension by a factor of about 2-fold at a peptide mole fraction of around 0.01 (Evans & Needham, 1987). The relationship between membrane fusion and cubic phase formation has also been recently suggested from studies of phospholipase C-induced liposome fusion (Nieva et al., 1995).

Viral fusion is only one example of the many biological processes requiring membrane fusion, (White 1992). The central event during membrane fusion is the merger of two membranes, which requires a transient reorganization of membrane lipids. For this reason, the fusion of pure lipid model membranes is extensively studied. The liposome model with viral fusion peptides still retains many of the features of the biological fusion process. Thus, the conclusions from the present study may provide important information on the basic mechanism of biomembrane fusion.

ACKNOWLEDGMENT

We are very grateful to Dr. Arlene Rockwell of the Dupont Merck Pharmaceutical Co. for purifying the peptides used in this work by HPLC. We appreciate several helpful suggestions from Dr. David Siegel. We are also grateful to Drs. S. W. Hui and A. Sen for use of their X-ray equipment.

REFERENCES

Anderson, D. M., Gruner, S. M., & Leibler, S. (1988) *Proc. Natl. Acad. Sci. U.S.A. 85*, 5364−5368.
Bullough, P. A., Hughson, F. M., Skehel, J. J., & Wiley, D. C. (1984) *Nature 371*, 37−43.
Burger, K. N. J. (1997) in *Lipid Polymorphism and Membrane Properties* (Epand, R. M., Ed.) Academic Press, San Diego (in press).
Burger, K. N. J., & Verkleij, A. J. (1990) *Experientia 46*, 631−644.
Burger, K. N. J., Wharton, S. A., Demel, R. A., & Verkleij, A. J. (1991) *Biochemistry 30*, 11173−11180.
Carr, C. M., & Kim, P. S. (1993) *Cell 73*, 823−832.
Cheetham, J. J., Nir, S., Johnson, E., Flanagan, T. D., & Epand, R. M. (1994) *J. Biol. Chem. 268*, 5467−5472.
Chernomordik, L. (1996) *Chem. Phys. Lipids 81*, 203−213.
Chernomordik, L. V., Melikyan, G. B., & Chizmadzhev, Y. A. (1987) *Biochim. Biophys. Acta 906*, 309−352.
Colotto, A., Martin, I., Ruysschaert, J.-M., Sen, A., Hui, S. W., & Epand, R. M. (1996) *Biochemistry 35*, 980−989.
Durrer, P., Galli, C., Hoenke, S., Corti, C., Glück, R., Vorherr, T., & Brunner, J. (1996) *J. Biol. Chem. 271*, 13417−13421.
Düzgünes, N., & Shavnin, S. A. (1992) *J. Membr. Biol. 128*, 71−80.
Ellens, H., Siegel, D. P., Alford, D., Yeagle, P. L., Boni, L., Lis, L. J., Quinn, P. J., & Bentz, J. (1989) *Biochemistry 28*, 3692−3703.
Epand, R. F., Martin, I., Ruysschaert, J.-M., & Epand, R. M. (1994) *Biochem. Biophys. Res. Commun. 205*, 1938−1943.
Epand, R. M. (1992) in *Membrane Interactions of HIV: Implications for Pathogenesis and Therapy in AIDS* (Aloia, R. C., & Curtain, C. C., Eds.) pp 99−112, Wiley-Liss, New York.
Epand, R. M., & Epand, R. F. (1988) *Chem. Phys. Lipids 49*, 101−104.
Epand, R. M., & Epand, R. F. (1994) *Biochem. Biophys. Res. Commun. 202*, 1420−1425.
Epand, R. M., Cheetham, J. J., Epand, R. F., Yeagle, P. L., Richardson, C. D., Rockwell, A., & DeGrado, W. F. (1992) *Biopolymers 21*, 309−314.
Epand, R. M., Nir, S., Parolin, M., & Flanagan, T. D. (1995) *Biochemistry 34*, 1084−1089.
Epand, R. M., Fuller, N., & Rand, R. P. (1996) *Biophys. J. 71*, 1806−1810.
Evans, E., & Needham, D. (1987) *J. Phys. Chem. 91*, 4219−4228.
Gagne, J., Stamatatos, L., Diacobo, T., Hui, S. W., Yeagle, P. L., & Silvius, J. R. (1985) *Biochemistry 24*, 4400−4408.
Gething, M.-J., Doms, R. W., York, D., & White, J. (1986) *J. Cell Biol. 102*, 11−23.
Gruner, S. M., Tate, M. W., Kirk, G. L., So, P. T., Turner, D. C., Keane, D. T., Tilcock, C. P., & Cullis, P. R. (1988) *Biochemistry 27*, 2853−2866.
Haywood, A. M., & Boyer, B. P. (1985) *Proc. Natl. Acad. Sci. U.S.A. 82*, 4611−4615.

Hui, S. W., Stewart, T. P., & Boni, L. T. (1983) *Chem. Phys. Lipids 33*, 113−126.
Ishiguro, R., Matsumoto, M., & Takahashi, S. (1996) *Biochemistry 35*, 4976−4983.
Kim, C.-H., Macosko, J. C., Yu, Y. G., & Shin, Y.-K. (1996) *Biochemistry 35*, 5359−5365.
Lünberg, J., Martin, I., Nüssler, F., Ruysschaert, J.-M., & Herrmann, A. (1995) *J. Biol. Chem. 270*, 27606−27614.
Markin, V. S., Kozlov, M. M., & Borovjagin, V. L. (1984) *Gen. Physiol. Biophys. 5*, 361−377.
Martin, I., Dubois, M.-C., Defrise-Quertain, F., Saermark, T., Burny, A., Brasseur, R., & Ruysschaert, J.-M. (1994) *J. Virol. 68*, 1139−1148.
Murata, M., Kagiwada, S., Hishida, R., Ishiguro, R., Ohnishi, S., & Takahashi, S. (1991) *Biochem. Biophys. Res. Commun. 179*, 1050−1055.
Nieva, J. L., Alonso, A., Basáñez, G., Goñi, F. M., Gulik, A., Vargas, R., & Luzzati, V. (1995) *FEBS Lett. 368*, 143−147.
Rafalski, M., Ortiz, A., Rockwell, A., van Ginkel, L. C., Lear, J. D., DeGrado, W. F., & Wilschut, J. (1991) *Biochemistry 30*, 10211−10220.
Rand, R. P., Fuller, N., Parsegian, V. A., & Rau, D. C. (1988) *Biochemistry 27*, 7711−7722.
Schoch, C., & Blumenthal, R. (1993) *J. Biol. Chem. 268*, 9267−9274.
Sen, A., Hui, S. W., Mannock, D. A., Lewis, R. N. A. H., & McElhaney, R. N. (1990) *Biochemistry 29*, 7799−7804.
Shyamsunder, E., Gruner, S. M., Tate, M. W., Turner, D. C., So, P. T., & Tilcock, C. P. (1988) *Biochemistry 27*, 2332−2336.
Siegel, D. P. (1986) *Chem. Phys. Lipids 42*, 279−301.
Siegel, D. P. (1993) *Biophys. J. 65*, 2124−2140.
Siegel, D. P., & Banschbach, J. L. (1990) *Biochemistry 29*, 5975−5981.
Siegel, D. P., & Epand, R. M. (1997) *Biophys. J.*, *72*, A302.
Siegel, D. P., Burns, J. L., Chestnut, M. H., & Talmon, Y. (1989) *Biophys. J. 56*, 161−169.
Siegel, D. P., Green, W. J., & Talmon, Y. (1994) *Biophys. J. 66*, 402−414.
Silvius, J. R., & Brown, P. M. (1986) *Biochemistry 25*, 4249−4258.
Stegmann, T. (1993) *J. Biol. Chem. 268*, 1716−1722.
Stegmann, T., Doms, R. W., & Helenius, A. (1989) *Annu. Rev. Biophys. Biophys. Chem. 18*, 187−211.
Tatulian, S. A., Hinterdorfer, P., Baber, G., & Tamm, L. K. (1995) *EMBO J. 14*, 5514−5523.
van Gorkom, L. C. M., Nie, S.-Q., & Epand, R. M. (1992) *Biochemistry 31*, 671−677.
Watowich, S. J., Skehel, J. J., & Wiley, D. C. (1994) *Structure 2*, 719−731.
Wharton, S. A., Martin, S. R., Ruigrok, R. W. H., Skehel, J. J., & Wiley, D. C. (1988) *J. Gen. Virol. 69*, 1847−1857.
White, J. M. (1992) *Science 258*, 917−924.
Wilson, I. A., Skehel, J. J., & Wiley, D. C. (1981) *Nature 289*, 368−373.

BI970382U